The Hierarchy of Structural Transitions Induced in Cytochrome *c* by Anionic Phospholipids Determines Its Peroxidase Activation and Selective Peroxidation during Apoptosis in Cells†

Alexander A. Kapralov,‡ Igor V. Kurnikov,‡ Irina I. Vlasova,‡,§ Natalia A. Belikova,‡ Vladimir A. Tyurin,‡ Liana V. Basova,‡ Quing Zhao,‡ Yulia Y. Tyurina,‡ Jianfei Jiang,‡ Hulya Bayir,‡,|| Yuri A. Vladimirov,‡,§ and Valerian E. Kagan*,‡

Center for Free Radical and Antioxidant Health, Department of Environmental and Occupational Health, University of Pittsburgh, Safar Center for Resuscitation Research, University of Pittsburgh Medical Center, and Department of Critical Care Medicine, University of Pittsburgh, Pittsburgh, Pennsylvania 15260, and The Research Institute of Physico-Chemical Medicine, Moscow 119992, Russia

Received June 22, 2007; Revised Manuscript Received September 25, 2007

ABSTRACT: Activation of peroxidase catalytic function of cytochrome *c* (cyt *c*) by anionic lipids is associated with destabilization of its tertiary structure. We studied effects of several anionic phospholipids on the protein structure by monitoring (1) Trp_{59} fluorescence, (2) Fe−S(Met_{80}) absorbance at 695 nm, and (3) EPR of heme nitrosylation. Peroxidase activity was probed using several substrates and protein-derived radicals. Peroxidase activation of cyt *c* did not require complete protein unfolding or breakage of the Fe−S(Met_{80}) bond. The activation energy of cyt *c* peroxidase changed in parallel with stability energies of structural regions of the protein probed spectroscopically. Cardiolipin (CL) and phosphatidic acid (PA) were most effective in inducing cyt *c* peroxidase activity. Phosphatidylserine (PS) and phosphatidylinositol bisphosphate (PIP_2) displayed a significant but much weaker capacity to destabilize the protein and induce peroxidase activity. Phosphatidylinositol trisphosphate (PIP_3) appeared to be a stronger inducer of cyt *c* structural changes than PIP_2, indicating a role for the negatively charged extra phosphate group. Comparison of cyt *c*-deficient HeLa cells and mouse embryonic cells with those expressing a full complement of cyt *c* demonstrated the involvement of cyt *c* peroxidase activity in selective catalysis of peroxidation of CL, PS, and PI, which corresponded to the potency of these lipids in inducing cyt *c*'s structural destabilization.

Post-translational covalent modifications of proteins are critical to coordination of the compartmentalized metabolism and destiny of proteins in cells. Regulation of catalytic functions by phosphorylation and S-nitrosation, targeted change in the location and intramembrane topography of proteins through ribosylation, palmitoylation/myristoylation, or phospholipidation, and even marking proteins for degradation and elimination via ubiquitinylation are only few of many examples of the importance of the hydrophobic−hydrophilic balance in the control of association of proteins with different membranes. In addition to these chemical covalent modifications of proteins, their functions can be effectively regulated by a broad range of noncovalent interactions with membranes (*1*, *2*).

More than half of all proteins in living cells are associated with lipid membranes. Membrane proteins are subdivided into integral (permanently and tightly attached to the membrane) and peripheral proteins interacting with the membranes only under certain conditions. Studies of peripheral membrane proteins are particularly challenging because of the transient nature of protein−lipid complexes. Lipid−protein interactions can also be modulated by alterations of external conditions such as pH, concentrations of divalent ions, or changes in lipid composition. The nature of lipid−protein interactions is still poorly understood, and quantitative

† This work was supported by NIH Grants U19 AI068021, HL 070807, NIOSH OH008282, and AHA0535365N, Pennsylvania Department of Health Grant SAP 4100027294, and RFFI (Russian Foundation of Fundamental Investigations) Grants 05-04-49765-a and 05-04-08101.

* To whom correspondence should be addressed: Department of Environmental and Occupational Health, Graduate School of Public Health, University of Pittsburgh, 100 Technology Dr., Suite 350, Pittsburgh, PA 15219-3130. Telephone: (412) 624-9479. Fax: (412) 624-9361. E-mail: kagan@pitt.edu.

‡ Department of Environmental and Occupational Health, University of Pittsburgh.

§ The Research Institute of Physico-Chemical Medicine.

|| University of Pittsburgh Medical Center and Department of Critical Care Medicine, University of Pittsburgh.

[1] Abbreviations: cyt *c*, cytochrome *c*; CL, cardiolipin; DEANOate, 1,1-diethyl-2-hydroxy-2-nitrosohydrazine; DMPO, 5,5-dimethyl-1-pyrroline *N*-oxide; DOPA, 1,2-dioleoyl-*sn*-glycero-3-phosphate (phosphatidic acid); DOPC, dioleoyl-*sn*-glycero-3-phosphatidylcholine; DOPS, 1,2-dioleoyl-*sn*-glycero-3-phospho-L-serine; DTPA, diethylenetriaminepentaacetic acid; EPR, electron paramagnetic resonance; GuHCl, guanidine hydrochloride; HPLC, high-pressure liquid chromatography; H_2O_2, hydrogen peroxide; MECs, mouse embryonic cells; MS, mass spectroscopy; PA, phosphatidic acid; PC, phosphatidylcholine; PI, phosphoinositol; PIP_2, 1,2-dioleoyl-*sn*-glycero-3-phosphoinositol 4,5-bisphosphate; PIP_3, 1,2-dioleoyl-*sn*-glycero-3-phosphoinositol 3,4,5-trisphosphate; PS, phosphatidylserine; TOCL, 1,1′,2,2′-tetraoleoyl cardiolipin.

10.1021/bi701237b CCC: $37.00
Published on Web 11/16/2007

analyses of physical factors causing association of proteins with lipid membranes and changes in their properties are rare (*3*, *4*).

An interesting case of a lipid-dependent modulation of protein function, loss of an electron-transport function and gain of a peroxidase catalytic function, is presented by a ubiquitous mitochondrial electron transport protein, cytochrome *c* (cyt *c*).[1] Normally, cyt *c* molecules are located in the intermembrane space of mitochondria and are loosely bound to the mitochondrial membranes by electrostatic forces. Thus, cyt *c* can be classified as a peripheral membrane protein. An increased content of a negatively charged cardiolipin (CL) in the outer leaflet of the inner membrane and the inner leaflet of the outer membrane, believed to occur early in apoptosis (*5*, *6*), increases the strength of cyt *c*−membrane interactions, destabilizes the protein tertiary structure, and results in a dramatically increased peroxidase activity (*7*−*9*). The peroxidase activity of cyt *c* is reportedly associated with selective oxidation of mitochondrial CL that further contributes to the execution of apoptosis (*10*). The spike in the peroxidase activity can be associated with an increased accessibility of a catalytic iron atom of the heme prosthetic group for hydrogen peroxide molecules. In solution, stability and unfolding of cyt *c* were extensively studied using deuterium exchange (*11*) and other experimental techniques (*12*−*15*). It was found that stabilities of different regions of the protein vary considerably: five distinct domains of cyt *c* were identified with stability energies ranging from 5 to 12 kcal/mol (*16*−*18*). Because the peroxidase catalytic function of cyt *c* in solution has been associated with an activation energy of ∼3.8 kcal/mol (*19*), one can predict that a small substrate molecule, H_2O_2, can access heme iron without substantial changes in the overall cyt *c*'s structure. Lipid-induced structural rearrangements of the cyt *c* molecule leading to its unfolding and conversion into a peroxidase remain poorly understood (*9*, *10*, *20*−*22*).

The protein regions may be destabilized differently by lipids with different chemical compositions due to specific protein−lipid interactions. Accordingly, lipid membranes may differ in their ability to induce peroxidase activity of cyt *c*. Protein−lipid interactions are complex, and multiple factors can contribute to the difference in the unfolding capacity of the lipids. Electrostatic forces are one of the major factors that govern protein−lipid interactions. Positively charged cyt *c* molecules (the net charge of +8e at pH 7.0) strongly interact with anionic membranes electrostatically, and this is apparently the main reason why anionic lipids are much stronger inducers of cyt *c* structural changes and peroxidase activity than noncharged (zwitterionic) lipids such as phosphatidylcholine (PC) (*23*−*25*). Electrostatic interactions attract cyt *c* molecules to anionic membranes and thus reduce their mobility (translational entropy), shifting the equilibrium toward the membrane-incorporated, denatured state of the protein. Direct electrostatic interactions between cyt *c* and lipid membranes, however, are not the only factor that affects unfolding of the protein. Hydrophobic interactions between nonpolar acyl residues of the lipid molecules and nonpolar regions of cyt *c* (normally buried inside the protein) are responsible for changes in the protein conformation. Alterations in saturation of the lipid acyl chains were shown to have a dramatic effect on cyt *c* unfolding. Thus, monounsaturated tetraoleoyl cardiolipin (TOCL) was found to be a much stronger inducer of cyt *c* conformational changes than saturated tetramyristoyl cardiolipin (TMCL), and polyunsaturated tetralinoleoyl cardiolipin (TLCL) appeared to be an even stronger cyt *c* denaturating agent than TOCL (*9*). Hydrogen bonding and other interactions between cyt *c* and polar lipid headgroups can significantly influence interactions of cyt *c* with membranes and lead to additional sensitivity of the protein structure destabilization to the chemical composition of the membranes. However, very little information is currently available on these interactions.

Because several anionic phospholipids can potentially interact with cyt *c* both within the mitochondria and in extramitochondrial compartments after its release during apoptosis, we compared the ability of several lipids with different headgroups in their ability to induce cyt *c* peroxidase activity and conformational changes. We used TOCL and dioleoylphosphatidylserine (DOPS) as two nonoxidizable variants of CL and phosphatidylserine (PS) which were previously found to activate cyt *c*'s peroxidase function in mitochondrial and extramitochondrial locations, respectively (*9*, *26*). The choice of phosphatidic acid (PA), in addition to CL and PS, was due to the fact that the structure of its headgroup is close to that of CL, but PA differs in the number of acyl chains, thus allowing the evaluation of the significance of the lipid structure in its protein unfolding properties. Moreover, PA has been demonstrated to partially substitute for CL deficiency in genetically manipulated (CL-deficient) cells (*27*). The comparison of dioleoyl-glycero-3-phosphoinositol 4,5-bisphosphate (PIP_2) and dioleoyl-glycero-3-phosphoinositol 3,4,5-trisphosphate (PIP_3), differing by only one phosphate group, was instrumental in identifying the effect of the single negative charge in the headgroup on its protein destabilization properties. Saturation of acyl chains can indeed change the unfolding properties of lipids. Since this work is focused on the effect of the structure of the headgroups in protein unfolding, we employed phospholipids with identical nonoxidizable monounsaturated acyl residues. The lipid choice was also affected by the fact that polyunsaturated phospholipids are good substrates for the peroxidase activity of cyt *c*, capable of competing with etoposide and Amplex Red and masking the true peroxidase activity of cyt *c*−lipid complexes toward these substrates.

In this work, we attempted to address three major questions.

(1) How effective are different physiologically relevant anionic phospholipids in inducing structural transitions as they relate to peroxidase activation of cyt *c*?

(2) What are the structural requirements for the anionic phospholipid-induced conversion of cyt *c* from an electron transporter into a peroxidase?

(3) To what extent is the peroxidase activity of cyt *c* realized in oxidation of anionic phospholipids in cells exposed to oxidative challenge (H_2O_2) or proapoptotic stimulation (actinomycin D)?

EXPERIMENTAL PROCEDURES

Materials. Horse heart cytochrome *c* (cyt *c*, type C-7752, >95%), diethylenetriaminepentaacetic acid (DTPA), 5,5-dimethyl-1-pyrroline *N*-oxide (DMPO), etoposide (demethylepipodophyllotoxin ethyldieneglucopyranoside), guanidine hydrochloride (GuHCl), and hydrogen peroxide (H_2O_2) were

purchased from Sigma-Aldrich (St. Louis, MO). 1,2-Dioleoyl-*sn*-glycero-3-phosphocholine (DOPC), 1,1′,2,2′-tetraoleoyl cardiolipin (TOCL), 1,2-dioleoyl-*sn*-glycero-3-phospho-L-serine (DOPS), 1,2-dioleoyl-*sn*-glycero-3-phosphoinositol 4,5-bisphosphate (PIP_2), 1,2-dioleoyl-*sn*-glycero-3-phosphoinositol 3,4,5-trisphosphate (PIP_3), and phosphatidic acid (1,2-dioleoyl-*sn*-glycero-3-phosphate) (DOPA) were purchased from Avanti Polar Lipids (Albaster, AL). The NO donors 1,1-diethyl-2-hydroxy-2-nitrosohydrazine (diethylamine NONOate; DEANOate) and rabbit DMPO nitrone adduct polyclonal antiserum were obtained from Cayman Chemical Co. (Ann Arbor, MI). Mouse anti-cyt *c* antibody (clone 7H8.2C12) was obtained from BD Biosciences (Franklin Lakes, NJ); goat anti-mouse HRP-conjugated antiserum and goat anti-rabbit alkaline phosphatase (AP)-conjugated antiserum were purchased from Pierce (Rockford, IL).

Small unilamellar liposomes were prepared from DOPC and anionic phospholipids (1:1 ratio) by sonication in HEPES buffer [20 mM with 100 μM DTPA (pH 7.4)].

Low-Temperature EPR Measurements. EPR spectra were recorded on a JEOL-REIX spectrometer with 100 kHz modulation (JEOL, Kyoto, Japan). For cyt *c* nitrosylation, cyt *c* (50 μM) was preincubated with liposomes in the presence of 500 μM ascorbate at room temperature (RT) to obtain ferro-cyt *c*; then 500 μM DEANOate was added, and the incubation was continued for 15 min. The reaction was stopped by freezing the samples in liquid nitrogen. The EPR spectra of nitrosylated cyt *c* were measured at 77 K under the following instrumental settings: center field, 3200 G; scan range, 500 G; field modulation, 5 G; microwave power, 10 mW; time constant, 0.1 s; scan time, 4 min; receiver gain, 5×10^2. The contribution of the hexacoordinate NO−heme complex in the EPR spectrum of nitrosylated cyt *c* was estimated by subtracting the spectrum of the pentacoordinate form of the NO−cyt *c* complex from the total spectrum of nitrosylated cyt *c* followed by the integration of each spectrum. The spectrum of the pentacoordinate NO−heme complex was measured in the presence of a NO donor DEANOate and a 100-fold excess of DOPA.

EPR spectra of protein-derived radicals were assessed after the addition of H_2O_2 (500 μM) to cyt *c* (100 μM) incubated with liposomes at RT. The reaction was stopped after 20 s by freezing the samples in liquid nitrogen. EPR spectra from frozen samples were recorded at 77 K under the following conditions: center field, 3230 G; sweep width, 100 G; field modulation, 5 G; microwave power, 1 mW; receiver gain, 10^3; time constant, 0.1 s; time scan, 4 min.

Peroxidase Activity Measurements. EPR spectra of etoposide phenoxyl radical were recorded at 25 °C in gas-permeable Teflon tubing (inner diameter, 0.8 mm; thickness, 0.013; Alpha Wire Corp., Elizabeth, NJ). The tubing (length, ~6 cm) was filled with 60 μL of sample, double-folded, and placed in an open 3.0 mm (internal diameter) EPR quartz tube. The spectra were recorded under the following EPR conditions: center field, 3350 G; sweep width, 50 G; microwave power, 10 mW; field modulation, 0.5 G; receiver gain, 5×10; time constant, 0.03 s; scan time, 8 min. The magnitude of the EPR signal of etoposide radical was measured 1 min after the addition of 100 μM H_2O_2 to the 5 μM cyt *c*/phospholipid and 100 μM etoposide solution; 100 AU (arbitrary units) of EPR signal corresponds to 6.5 μM etoposide radical [as calculated by the comparison with the EPR spectrum of 2 μM 2,2,6,6-tetramethylpiperidine *N*-oxide free radical (TEMPO)].

Assessment of peroxidase activity with Amplex Red was performed using the fluorescence of resorufin (oxidation product of Amplex Red) (λ_{ex} = 570 nm; λ_{em} = 585 nm); 0.5 μM cyt *c* was incubated with a different amount of lipids for 10 min. Then 50 μM Amplex Red and 25 μM H_2O_2 were added, and the incubation proceeded for an additional 30 min.

Assessments of peroxidase activity based on H_2O_2-induced oxidation of luminol to yield a chemiluminescence response were performed for 10 μM cyt *c* in the presence of 50-, 100-, and 200-fold molar excesses of anionic lipids, 500 μM luminol, and 100 μM H_2O_2.

Tryptophan 59 Fluorescence. The Trp_{59} fluorescence of cyt *c* in the presence and absence of liposomes was measured on an RF-5301 PC spectrofluorometer (Shimadzu) using standard quartz cuvettes with an optical path length of 1 cm. The excitation wavelength was 293 nm; the emission spectra were recorded in 300−500 nm regions. The concentration of cyt *c* was 5 μM. Incubation of the cyt *c*−liposome complex lasted for 15 min.

Absorbance Spectroscopy. Optical spectra were recorded on a UV160U spectrophotometer (Shimadzu) in 50 μL cuvettes as described in ref *9*. The concentration of cyt *c* was 50 μM.

Lipid Extraction and Two-Dimensional (2D) HPTLC Analysis. Total lipids were extracted from intact cells or mitochondria using the Folch procedure as previously described (*28*). Lipid extracts were separated and analyzed by 2D HPTLC as described in ref *29*. Lipid phosphorus was assessed by a micro method (*30*).

Phospholipid hydroperoxides were assessed by fluorescence HPLC of products formed in microperoxidase 11-catalyzed reaction with a fluorogenic substrate, Amplex Red, *N*-acetyl-3,7-dihydroxyphenoxazine (Molecular Probes, Eugene, OR) (*10*). Phospholipids were hydrolyzed by pancreatic phospholipase A_2 (2 units/mL) in 25 mM phosphate buffer containing 1.0 mM $CaCl_2$, 0.5 mM EDTA, and 0.5 mM SDS (pH 8.0 at RT for 30 min). After that, Amplex Red and microperoxidase 11 were added and samples were incubated at 4 °C for 40 min. A Shimadzu LC-100AT vp HPLC system equipped with a fluorescence detector (RF-10Axl) and an autosampler (SIL-10AD vp) was used for the analysis of products separated by an Eclipse XDB-C18 column (5 μm, 150 mm × 4.6 mm). The mobile phase was composed of 25 mM phosphate buffer (pH 7.0) and methanol (60:40, v/v).

Mass spectra of phospholipids were analyzed by direct infusion into an LXQ quadrupole linear ion trap mass spectrometer (Thermo Electron, San Jose, CA). Samples after 2D HPTLC separation were collected, evaporated under N_2, resuspended in a 1:2 (v/v) chloroform/methanol mixture (20 pmol/μL), and directly utilized for acquisition of electrospray ionization (ESI) mass spectra at a flow rate of 5 μL/min. The electrospray probe was operated at a voltage differential of −3.5 to 5.0 kV in the negative or positive ion mode. The source temperature was maintained at 150 °C. To determine the fatty acid composition of phospholipid, the pulsed-Q dissociation (PQD) technique was applied with a relative collision energy ranging from 20 to 40% and a *q* value of 0.7.

PAGE and Western Blotting Analysis. cyt *c* (1.5 μM) was incubated with liposomes in 20 mM HEPES (pH 7.4) for 15 min at RT. Then samples were transferred to a water bath and incubated at 37 °C for an additional 1 h. H_2O_2 (25 μM) was added every 15 min. Proteins were separated by 12.5% SDS−PAGE in Tris-glycine buffer. The separated proteins were electrotransferred to a nitrocellulose membrane. After the samples had been blocked with 5% nonfat milk dissolved in phosphate-buffered saline, Tween 20 (0.05%) (PBS-T) (for cyt *c* detection) or Tris-buffered saline with Tween 20 containing 0.25% casein (TBS-T) (for DMPO detection) for 1 h was incubated overnight at 4 °C with primary antibodies (anti-cyt *c* or anti-DMPO antibodies). The membranes were washed several times followed by incubation with HRP-conjugated goat anti-mouse antiserum (for cyt *c* detection) or AP-conjugated goat anti-rabbit antiserum (for DMPO detection) for 60 min at RT. The protein bands were visualized by using SuperSignal West Pico Chemiluminescent Substrate (Pierce, Rockford, IL) for the HRP-conjugated secondary antibody or Lumi-Phos WB (Pierce) for the AP-conjugated secondary antibody as described by manufacturer. The density of bands was determined by scanning with Epi Chemi II Darkroom (UVP BioImaging Systems, Upland, CA).

Cell Culture. Mouse embryonic cyt $c^{-/-}$ cells (ATCC) and cyt $c^{+/+}$ cells (courtesy of Xiaodong Wang, University of Texas, Dallas, TX) were cultured in DMEM supplemented with 15% FBS, 25 mM HEPES, 50 mg/L uridine, 110 mg/L pyruvate, 2 mM glutamine, 1× nonessential amino acids, 2′-mercaptoethanol, 0.5 × 10^6 units/L mouse leukemia inhibitory factor, 100 units/mL penicillin, and 100 mg/mL streptomycin. HeLa cells were purchased from ATCC and cultured in the same conditioned medium as mouse embryonic cells but without leukemia inhibitory factor. cyt $c^{-/-}$ and cyt $c^{+/+}$ mouse embryonic cells were exposed to ActD (100 ng/mL) for 16 h at 37 °C.

Statistical Analysis. Data are expressed as means (standard deviation of at least triplicate determinations). Changes in variables were analyzed by a one-way ANOVA for multiple comparisons. Differences were considered significant at $p < 0.05$.

RESULTS

We used three different approaches to monitor structural changes of cyt *c* during its interactions with anionic lipids: (1) assessments of Trp_{59} fluorescence, (2) measurements of optical absorbance at 695 nm, and (3) EPR measurements of heme nitrosylation whereby each of the methods probes different regions of the protein. Five different anionic phospholipids used in the study (see Figure 1) were mixed with zwitterionic DOPC at a ratio of 1:1. All experiments were performed in 20 mM HEPES-Na buffer (pH 7.4) containing 100 μM DTPA.

Trp_{59} Fluorescence. The intrinsic protein fluorescence, arising primarily from a single tryptophan at position 59, is a very sensitive probe for monitoring the overall conformation of cyt *c*. In the native state, fluorescence of Trp_{59} is almost completely quenched due to its proximity to the heme group (*31*).

For all lipids tested, the fluorescence of cyt *c* increased with an increasing lipid:protein ratio, thus showing the diminished quenching due to unfolding of the protein (Figure 2A). The anionic lipids studied clearly differed in their ability to unfold cyt *c*. At high concentrations of TOCL-, DOPA-, and DOPS-containing liposomes, cyt *c* fluorescence intensity reached a saturation level that was close to the fluorescence of cyt *c* fully unfolded by guanidine hydrochloride (6 M). The Trp_{59} fluorescence intensity saturation level for PIP_2 and PIP_3 was ~2 times lower than that for fully unfolded (by guanidine hydrochloride) cyt *c*, indicating that cyt *c* is present in a more compact state in PIP_2- and PIP_3-containing membranes.

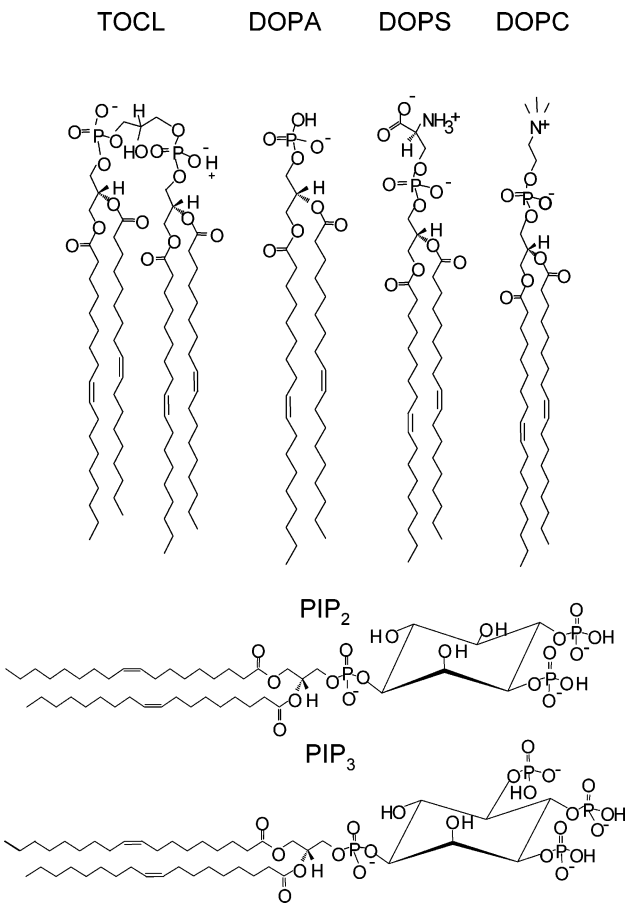

FIGURE 1: Structural formulas of anionic lipids TOCL, DOPA, DOPS, DOPC, PIP_2, and PIP_3. Phospholipids are presented in forms in which they existed at pH 7.4. In accord with the pK_a values for the phospholipid headgroups, they change their ionization state at near-physiological pH: $pK_{1R-HPO_4} = 3.0$ and $pK_{2R-HPO_4} = 8.0$ for TOCL, $pK_{R-HPO_4} = 3$ and $pK_{R-PO_4} = 8$ (0.1 M NaCl) for DOPA, and $pK_{R-HPO_4} = 2.6$ and $pK_{COO^-} = 5.5$ (0.1 M NaCl) for DOPS.

We established that two independent parameters are essential to adequately describe activation of Trp_{59} fluorescence of cyt *c* by phospholipids. The saturation level parameter describes maximal unfolding of cyt *c*−lipid complexes achieved at high lipid:protein ratios. This parameter changed significantly in response to different lipids, indicating that cyt *c* adopts different conformations upon interaction with these phospholipids. Half-maximal values characterize lipid:protein ratios corresponding to the point when the unfolding reached half-maximal activity; this parameter varied significantly for phospholipids that were studied. On the basis of the ability to induce half-maximum conformational changes of cyt *c* assessed by the Trp_{59} fluorescence, PIP_3 appeared to be the strongest agent (the

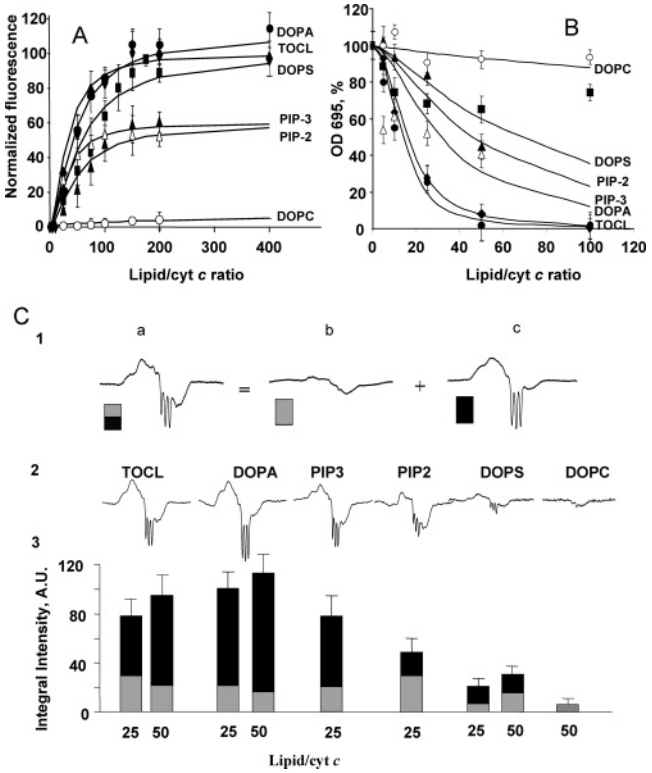

FIGURE 2: Structural changes of cyt *c* upon its binding to anionic lipids. (A) Anionic lipids enhance the fluorescence of Trp_{59}. Dependence of the ratio of cyt *c* Trp_{59} fluorescence to fluorescence of GuHCl (6 M)-unfolded cyt *c* ($\lambda_{ex} = 293$ nm; $\lambda_{em} = 340$ nm) on lipid:cyt *c* ratio [20 mM HEPES (pH 7.4)]. (B) Anionic lipids disrupt the Fe−S(Met_{80}) coordination bond. Dependence of the absorbance of the Fe−S(Met_{80}) bond ($\lambda = 695$ nm) on the lipid:cyt *c* ratio [20 mM HEPES (pH 7.4)]. (C) Anionic lipids facilitate cyt *c* nitrosylation as evidenced by EPR spectroscopy. EPR spectra of nitrosylated cyt *c*−lipid complexes formed in the presence of a NO donor, DEANOate. (1) Typical EPR spectra of nitrosylated cyt *c*: (a) superposition of signals from penta- and hexacoordinate NO−cyt *c* complexes, (b) hexacoordinate NO−cyt *c* complex, and (c) pentacoordinate NO−cyt *c* complex. (2) Typical EPR spectra obtained from cyt *c* nitrosylated in the presence of different anionic lipids. (3) Integral intensity of hexacoordinate and pentacoordinate components of the EPR spectra of cyt *c* nitrosylated in the presence of different anionic lipids.

half-maximal effect was achieved at a lipid:protein ratio of ~20). The half-maximal unfolding of cyt *c* by TOCL- and DOPA-containing membranes was achieved for these phospholipids only at lipid:protein ratios of ~45−50. DOPS caused a half-maximal fluorescence response at lipid:protein ratios of ~70−80, and PIP_2 did it at ~60. Importantly, liposomes prepared from noncharged DOPC did not detectably affect cyt *c* Trp_{59} fluorescence. Table 1 summarizes our results of evaluating how phospholipids ranked in their effectiveness to induce cyt *c* Trp_{59} fluorescence in terms of a maximal level of fluorescence (maximal unfolding) and in terms of the ability to achieve a half-maximal level of fluorescence (effectiveness of unfolding).

Absorbance at 695 nm. Another assay that we used to monitor unfolding of cyt *c* was the change in the characteristic absorbance band at 695 nm associated with an axial coordination of the heme iron in cyt *c* by the sulfur atom of Met_{80}. The Fe−S(Met_{80}) bond is not very strong (*32*), and Met_{80} is located in the region of the protein that is much less stable than the protein domain containing Trp_{59} (*16*, *17*). Incubation of cyt *c* with increasing amounts of phospholipids resulted in weakening of the 695 nm absorbance. TOCL and DOPA exhibited the strongest ability to disrupt the Fe−S(Met_{80}) bond completely, eliminating the 695 nm absorbance at a 50:1 lipid:protein ratio. The absorbance was decreased by 50% at lipid:protein ratios of 5−10 (i.e., at concentrations of these phospholipids much lower than those required for 50% reduction of Trp_{59} fluorescence). Similarly, relatively low concentrations of PIP_3 (lipid:protein ratio of 5−10) were required to disrupt 50% of Fe−S(Met_{80}) bonding. However, like its effects on Trp_{59} fluorescence, a further increase in the PIP_3:protein ratio resulted in almost no further decay of the 695 nm absorbance. This behavior is probably indicative of a compact state of cyt *c* formed in the complex with highly charged PIP_3 whereby the native Met ligation of heme is highly probable. DOPS and PIP_2 displayed a much poorer ability to diminish 695 nm absorbance (Figure 2B). Noncharged PC did not significantly affect the 695 nm absorbance. The relative abilities of phospholipids to reduce the absorbance at 695 nm and disruption of Fe−S(Met_{80}) bonds, in terms of the half-maximal efficiency of the absorbance decrease and maximal elimination of the absorbance and disruption of Fe−S(Met_{80}) bonds, are reported in Table 1.

Heme Nitrosylation. In the native conformation, the iron atom of cyt *c* is protected against interaction with small molecules such as NO, CO, and H_2O_2 by coordination with porphyrin and two axial ligands, Met_{80} and His_{18}. Destabilization of the tertiary structure of cyt *c* improves the access of heme iron to chemical interactions (*10*, *33*). We studied heme nitrosylation by nitric oxide to specifically probe phospholipid-induced changes in the cyt *c* tertiary structure, facilitating interactions of the heme moiety with small molecules. To this end, we used low-temperature (77 K) EPR spectroscopy to detect the formation of Fe−NO complexes. Only a weak predominantly hexacoordinate EPR signal was observed in the system containing the cyt *c*−Fe(II) complex and a NO donor, DEANOate. In the presence of anionic lipids, the magnitude of the EPR signal of nitrosylated heme increased in a concentration-dependent manner. Two types of heme−NO complexes were identified by EPR: a pentacoordinate complex [the second axial coordination position is vacant (Figure 2C, 1c)] characterized by a triple-line EPR signal at $g = 2.009$ with a splitting of 17 G and a hexacoordinate complex [the second axial position of heme is occupied by a new "non-native" ligand (Figure 2C, 1b)] (*33*, *34*). As established for TOCL and DOPA, an increase in the lipid:cyt *c* ratio resulted not only in increased amounts of nitrosylated cyt *c* but also in a larger contribution of the pentacoordinate form to the total signal of nitrosylated cyt *c*. As a measure of heme accessibility (and protein structure perturbation), we employed the magnitude of the total EPR signal with partially superimposed pentacoordinate and hexacoordinate species. The protein structure was most strongly perturbed by DOPA followed by TOCL and PIP_3, PIP_2, and DOPS. DOPC was ineffective in inducing enhanced heme−NO interactions (Figure 2C, 2 and 3). The order of potency of phospholipids in causing heme nitrosylation is presented in Table 1.

Peroxidase Activity. EPR spectroscopy of nitrosylated cyt *c*, optical spectroscopy, and measurements of Trp_{59} fluorescence demonstrated that interactions of cyt *c* with anionic

Table 1: Rank Order of Anionic Phospholipids of the Ability To Induce cyt *c* Conformational Changes and Peroxidase Activity Assessed by Different Methods

	TOCL	DOPA	PIP_3	PIP_2	DOPS	DOPC
Trp_{59} fluorescence[a] (lipid:protein ratio for half-maximal effect)	2−3 (45−50)	2−3 (45−50)	1 (20)	4−5 (60)	4−5 (70−80)	6
Trp_{59} fluorescence[a] (maximal fluorescence, normalized to fluorescence after unfolding by GuHCl)	1−3 (80−100)	1−3 (80−100)	4−5 (50)	4−5 (50)	1−3 (80−100)	6
absorbance at 695 nm[a] (lipid:protein ratio for half-maximal effect)	1−2 (5−10)	1−2 (5−10)	3 (5−10)	4−5 (25−30)	4−5 (25−30)	6
absorbance at 695 nm[a] (maximal absorbance decrease, %)	1−2 (100)	1−2 (100)	3 (50)	4−5 (30−40)	4−5 (30−40)	6
NO−heme binding[a]	2−3	1	2−3	4	5	6
peroxidase activity[a] (lipid:protein ratio for half-maximal effect)	1−2	1−2	3−5	3−5	3−5	6
peroxidase activity[a] (maximal activity)	1−2	1−2	3−5	3−5	3−5	6
formation of protein radicals[b]	1−2	1−2			3	4

[a] The effectiveness decreases in order from 1 to 6. The numbers in parentheses provide a quantitative estimate of the lipid strength (lipid:protein ratios of half-maximal fluorescence, maximal fluorescence, etc.). [b] The effectiveness decreases in order from 1 to 4 (formation of protein radicals was not studied for PIP_2 and PIP_3).

phospholipids induced protein unfolding accompanied by a loss of an axial ligand of heme iron and made it more accessible to small molecules like NO or possibly H_2O_2. An increased accessibility of the catalytic iron atom should cause an increase in the cyt *c* peroxidase activity. Indeed, addition of anionic phospholipids increased the peroxidase activity assessed by oxidation of three prototypical substrates: Amplex Red (accumulation of the oxidation product, resorufin, measured by its characteristic fluorescence), etoposide (time-dependent concentration of etoposide radical monitored by EPR) (Figure 3A), and luminol (assessed by the chemiluminescence of its oxidation products) (Figure 3B). All three methods yielded similar results and showed that TOCL and DOPA were much more effective than the other anionic phospholipids in inducing the peroxidase activity. Apparent strengths of phospholipids in inducing peroxidase activity of cyt *c* are presented in Table 1. At high lipid:protein ratios, the peroxidase activity reached a maximal value. Notably, the maximal values of the cyt *c* peroxidase activity varied for different phospholipids. The maximal peroxidase activity induced by TOCL and DOPA was ~3 times higher than that caused by DOPS, PIP_3, and PIP_2 as indicated in Table 1.

Formation of Protein-Derived Radicals of cyt c as a Function of Lipid:cyt c Ratio. Characteristic reactive intermediates of peroxidase-catalyzed reactions are protein-immobilized radicals, most commonly tyrosyl radicals (*35*−*37*). These radical intermediates can be detected by low-temperature EPR spectroscopy (*36*), as well as by the recently developed immuno-spin trapping technique (*37*, *38*). Both EPR spectra and immuno-spin trapping have been successfully used in studies of peroxidase activity of cyt *c* (*33*, *36*, *39*, *40*). Therefore, we employed EPR spectroscopy to characterize the ability of different anionic phospholipids to facilitate the H_2O_2-dependent production of cyt *c* protein-immobilized radicals. A typical low-temperature EPR spectrum (Figure 4A) obtained from an incubation system containing a cyt *c*/anionic phospholipid mixture and H_2O_2 represents the characteristic signal of protein-derived (tyrosyl) radicals of the activated peroxidase with a peak-to-trough width of ~16 G and a *g* factor of ~2.005 (*41*). Increasing the phospholipid:cyt *c* ratio resulted in an increased magnitude of the EPR signal of the protein-derived radicals. Table 1 shows the effectiveness of phospholipids in inducing the protein-derived radicals on the basis of the magnitudes of the observed EPR signals.

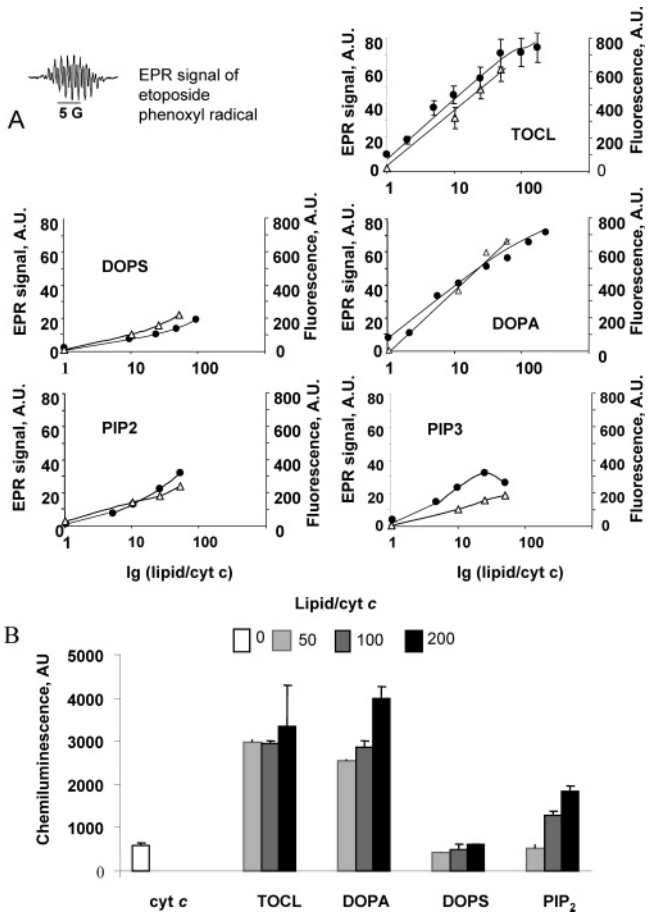

FIGURE 3: Interactions with anionic phospholipids induce peroxidase activity of cyt *c* assessed by H_2O_2-induced oxidation of three substrates. (A) Etoposide (monitored by EPR spectroscopy of etoposide one-electron oxidation product, phenoxyl radical) (●) and Amplex Red (measured by the fluorescence of its oxidation product, resorufin) (△). Insets show a typical EPR spectrum of etoposide phenoxyl radical. (B) Luminol (determined by the chemiluminescence response of oxidation products).

Recombination of protein-derived tyrosyl radicals, resulting from the peroxidase activity of cyt *c*, is known to cause

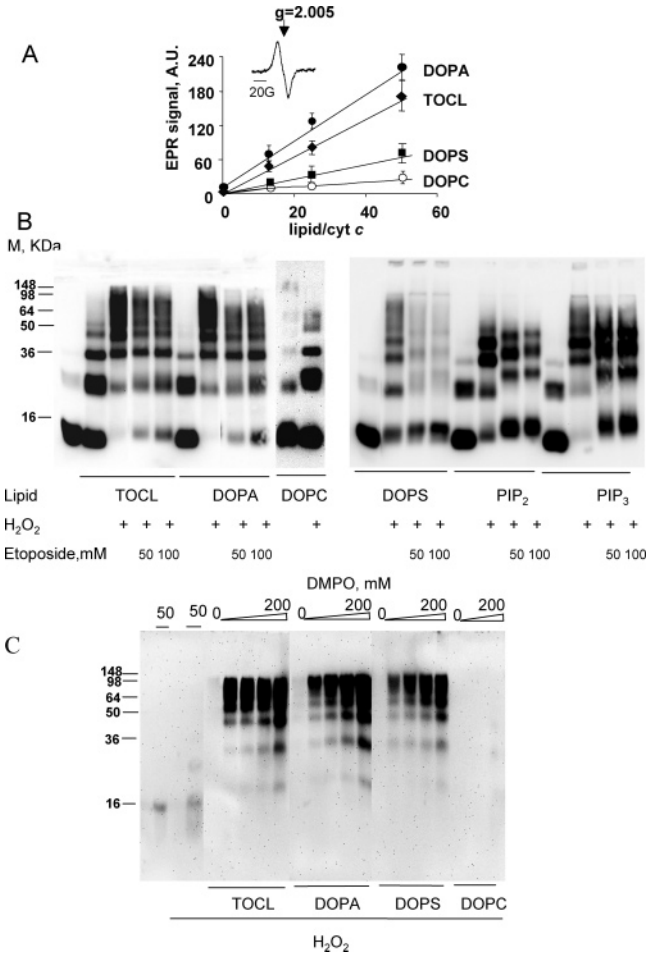

FIGURE 4: Production of protein-derived radicals and aggregation of cyt *c* as a result of incubation of cyt *c*−lipid complexes with H_2O_2. (A) Dependence of the magnitude of EPR signals of protein-derived radicals on the lipid:cyt *c* ratio. The inset shows a typical low-temperature EPR spectrum of protein-derived radicals formed 20 s after the addition of H_2O_2 to incubated liposomes cyt *c*. EPR spectra from frozen samples were detected at 77 K. (B) Oligomerization of cyt *c* due to recombination of protein-derived radicals. Western blotting of aggregates of cyt *c* formed after its incubation with phospholipid/H_2O_2 membranes. Note that addition of a peroxidase substrate etoposide results in inhibition of cyt *c* oligomerization. The molecular masses (kilodaltons) are indicated at the left. (C) Immuno-spin trapping detection of cyt *c*-derived radicals. Western blotting of H_2O_2-induced aggregates of cyt *c* formed in the presence of different anionic phospholipids using anti-DMPO antibody. The molecular masses (kilodaltons) are indicated at the left.

oligomerization of the protein via dityrosine cross-links (nondissociable by S−S reducing reagents) (*39*, *42*). Indeed, incubation of cyt *c* with anionic phospholipids in the presence of H_2O_2 resulted in the disappearance of its monomeric form and accumulation of oligomers (Figure 4B). On the basis of PAGE assessments of the remaining monomeric form of cyt *c*, the strengths of phospholipids in inducing peroxidase-dependent oligomerization of the protein ranked as follows: TOCL ∼ DOPA > PIP_3 > PIP_2 > DOPS ≫ DOPC. Notably, more effective phospholipids (TOCL and DOPA) caused accumulation of very high-molecular weight aggregates, while less potent phospholipids (PIP_3, DOPS, and PIP_2) induced the formation of di-, tri-, tetra-, and pentameric forms of cyt *c*. In line with the peroxidase mechanism of oligomerization, in the presence of increasing concentrations of a competitive substrate, a phenolic compound etoposide, H_2O_2-dependent aggregation/oligomerization of cyt *c* was progressively inhibited, resulting in partial preservation of its monomeric form.

When cyt *c*/anionic phospholipids were incubated with H_2O_2 in the presence of a spin trap, DMPO, immunoreactive protein-immobilized spin adducts were detected by anti-DMPO antibodies (Figure 4C). The protein-derived radicals were found in all oligomeric forms of the protein and were not observed in the cyt *c* monomers. Again, TOCL and DOPA were markedly more effective in inducing the protein-immobilized radicals than DOPS. No protein DMPO− adducts were observed when cyt *c*/DOPC phospholipids were co-incubated with H_2O_2 and DMPO.

H_2O_2-Induced Peroxidation of Phospholipids in Cells with Different Levels of cyt c. Our previous studies demonstrated that, in addition to model chemical substrates, natural polyunsaturated anionic phospholipids can be utilized as substrates by the peroxidase activity of their complexes with cyt *c*, resulting in the accumulation of respective phospholipid hydroperoxides (*9*, *10*). To evaluate the role of the peroxidase activity of cyt *c* in peroxidation of endogenous phospholipid substrates, we employed wild-type HeLa cells and a clone, HeLa 1.2 cells, in which the content of cyt *c* was knocked down by RNAi manipulations. The content of cyt *c* in HeLa 1.2 cells was ∼14% of its level in parental HeLa cells. We performed MS characterization of major molecular species of anionic phospholipids in HeLa cells and HeLa 1.2 cells (Figure 5A) and found them to be very similar. MS analysis of CL isolated from wild-type HeLa cells revealed three major molecular species at *m*/*z* 699.7, 712.7, and 725.7. As an example of structural analysis, the MS^2 spectrum of the dominating molecular ion $[M - H]^{2-}$ at *m*/*z* 725.6 is shown in Figure 5B. MS^2 fragmentation of CL species at *m*/*z* 725.6 resulted in the formation of typical product ions at *m*/*z* 279.2, 281.2, and 283.2 that corresponded to linoleic ($C_{18:2}$), oleic ($C_{18:1}$), and stearic ($C_{18:0}$) acids, respectively. Product ion at *m*/*z* 279.2 ($C_{18:2}$) was dominating after fragmentation. The lack of significant differences in molecular speciation of phospholipids between HeLa and Hela 1.2 cells suggests that any specific features of phospholipid oxidation may not be interpreted in terms of their random oxidizability.

To activate the peroxidase activity, the cells were incubated in the presence of H_2O_2 (500 μM, 16 h). We found that two anionic phospholipids, CL and PS, underwent significant peroxidation in wild-type HeLa cells but not in HeLa 1.2 cells (Figure 5C). CL oxidation was markedly stronger than that of PS. A slight, although statistically insignificant, PI oxidation was also observed in wild-type HeLa cells but not in HeLa 1.2 cells. PA oxidation in cells could not be assessed due to undetectably low levels of PA in both HeLa cells and HeLa 1.2 cells. No oxidation of more abundant but noncharged phospholipids, PC and PE, was detected in either HeLa cells or HeLa 1.2 cells. To characterize oxidized CL formed in mitochondria of HeLa cells in the course of the H_2O_2-driven reaction, we used ESI-MS analysis. The MS^2 spectrum of molecular ions of oxygenated CL at *m*/*z* 741.3 that originated from molecular species at *m*/*z* 725.6 is shown in Figure 5B. Pulsed-Q dissociation of the ion (*m*/*z* 741.3) yielded molecular ions of $C_{18:2}$ (*m*/*z* 279.3), $C_{18:1}$ (*m*/*z* 281.3), $C_{18:0}$ (*m*/*z* 283.3), and $C_{18:2}$-OOH (hydroperoxylinoleic acid,

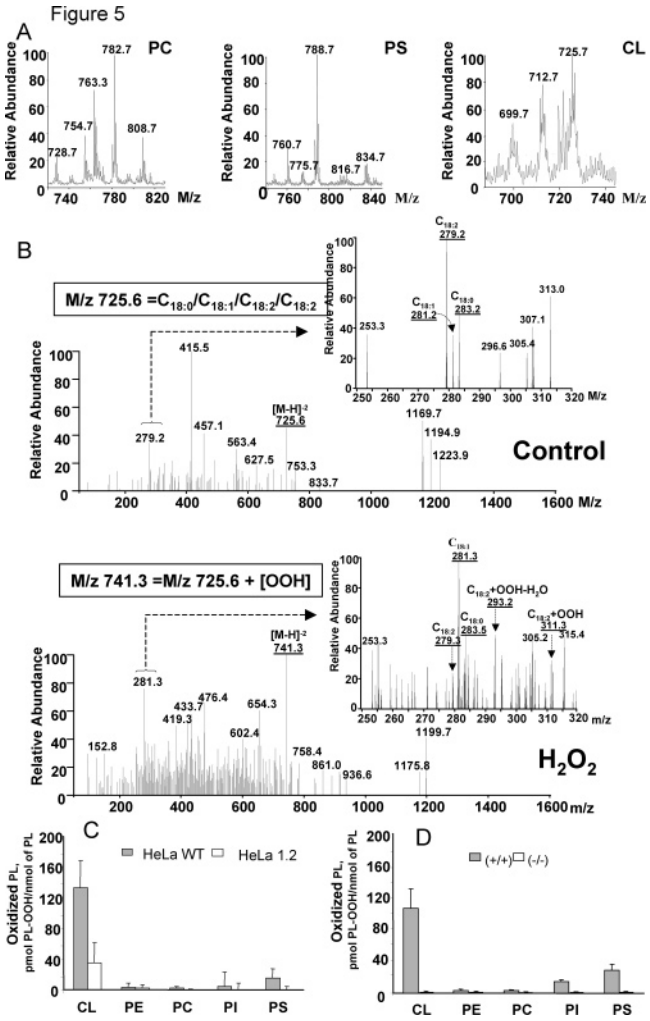

FIGURE 5: Characterization of H_2O_2-induced peroxidation of phospholipids in wild-type and cyt *c*-deficient cells. (A) MS analysis of major phospholipids from HeLa cells and HeLa 1.2 cells. Typical ESI mass spectra of PC (positive mode) as well as PS and CL (negative mode) obtained from HeLa 1.2 cells. Positive-ion MS spectra of PC showed that multiple molecular species, including species at *m*/*z* 754.7, 782.7, and 808.7. These molecular species contain fatty acid residues with two or more double bonds, including readily oxidizable, linoleic ($C_{18:2}$), linolenic ($C_{18:3}$), and arachidonic acids ($C_{20:4}$). Analysis of PS revealed three major molecular clusters at *m*/*z* 760.7, 788.7, and 834.7. One of them at *m*/*z* 834.7 includes a fatty acid residue with six double bonds, docosahexaenoic acid ($C_{22:6}$). ESI-MS analysis of CL molecular species revealed three major molecular ions at *m*/*z* 699.7, 712.7, and 725.7 for doubly charged ions which correspond to $(C_{16:0})_2/(C_{18:2})_2$ and $C_{16:0}/C_{16:1}/C_{18:1}/C_{18:2}$, $C_{16:0}/C_{18:1}/(C_{18:2})_2$ and $C_{16:1}/(C_{18:1})_2/C_{18:2}$, and $C_{18:1}/(C_{18:2})_3$, respectively. Thus, all molecular species of CL are polyunsaturated and contain readily oxidizable linoleic acid ($C_{18:2}$). (B) Negative ESI-MS^2 spectra of molecular ions of CL isolated from control and H_2O_2-treated HeLa cells. The molecular ion at *m*/*z* 741.2 corresponds to oxygenated CL, $(C_{18:2})/(C_{18:2}$-OOH$)/(C_{18:1})(C_{18:0})$, and originated from CL molecular species at *m*/*z* 725.6 $[(C_{18:2})_2/(C_{18:1})(C_{18:0})]$. Product ions at *m*/*z* 279.3, 281.3, 283.3, 311.3, and 293.3 formed after fragmentation of the molecular ion at *m*/*z* 741.3 corresponded to linoleic acid ($C_{18:2}$), oleic acid ($C_{18:1}$), stearic acid ($C_{18:0}$), hydroperoxylinoleic acid ($C_{18:2}$-OOH), and dehydrated hydroperoxylinoleic acid ($C_{18:2}$-OOH-H_2O), respectively. (C) Peroxidation of polyunsaturated phospholipids in HeLa cells and HeLa 1.2 cells challenged with hydrogen peroxide. (D) Peroxidation of polyunsaturated phospholipids in cyt $c^{+/+}$ and cyt $c^{-/-}$ mouse embryonic cells challenged with a pro-apoptotic agent, ActD.

m/*z* 311.3). A molecular ion at *m*/*z* 293.3 that originated from *m*/*z* 311.3 after dehydration was also observed in the MS^2 spectrum of oxidized CL at *m*/*z* 741.3 (Figure 5B). Thus, MS^n analysis revealed that $C_{18:2}$-OOH-CL was generated after exposure of cells to H_2O_2.

To further determine the extent to which selective oxidation of anionic phospholipids by the peroxidase activity of cyt *c* occurs during apoptosis, we utilized a different cell model, mouse embryonic cells with a full complement of cyt *c* (cyt $c^{+/+}$ MECs) and cyt *c*-deficient k/o mouse embryonic cells (cyt $c^{-/-}$ MECs) (Figure 5D). We found that stimulation of cyt $c^{+/+}$ cells with a nonoxidant pro-apoptotic agent, ActD, resulted in selective peroxidation of three anionic phospholipids which decreased in the following order: CL > PS > PI. More abundant phospholipids, PC and PE, did not undergo peroxidation. Typical accumulation of biomarkers of apoptosis was detectable in cyt $c^{+/+}$ MECs triggered with ActD. Most importantly, neither oxidation of anionic phospholipids nor the appearance of biomarkers of apoptosis was found in cyt $c^{-/-}$ MECs (*10*). However, ActD-induced production of superoxide, determined by the oxidation of dihydroethidium, was equally detectable in cyt $c^{+/+}$ and cyt $c^{-/-}$ MECs. MS analysis revealed no substantial differences in the patterns of major molecular species of oxidizable anionic phospholipids, CL, PS, and PI, between control (or untreated) cyt $c^{+/+}$ cells and cyt $c^{-/-}$ cells (data not shown).

DISCUSSION

Structural Transitions Required for the Activation of cyt c's Peroxidase Function by Anionic Phospholipids. Our results showed that although all anionic phospholipids were effective in destabilizing the tertiary structure of cyt *c* and inducing its peroxidase activity, their effectiveness greatly varied. Comparison of three structural parameters characterizing different regions of cyt *c* showed that the relative order of potency in which different phospholipids caused destabilization of protein structure varies significantly for different structural domains. Several assays revealed that TOCL and DOPA were most effective in unfolding cyt *c*. These lipids caused the highest levels of Trp_{59} fluorescence intensity, were most efficient in facilitating nitrosylation of the cyt *c* heme, and resulted in full disruption of the Fe−S(Met_{80}) bond. TOCL and DOPA with similar headgroups but different numbers of acyl chains exhibit very similar abilities to unfold cyt *c* and induce its peroxidase activity. This suggests that the charge distribution in the headgroup is an essential determinant of the unfolding efficiency of the lipids that were tested.

PIP_3 and PIP_2 caused cyt *c* to adopt a more compact structure that is characterized by a lower maximal Try_{59} fluorescence, partial preservation of the Fe−S(Met_{80}) bond (695 nm absorbance), and lower peroxidase activity compared with those of DOPA and TOCL. On the other hand, lower lipid:protein ratios were needed for PIP_3-containing liposomes than for DOPA and TOCL liposomes to denature cyt *c*. This is consistent with a relative compactness of cyt *c* structure in a complex with PIP_3 and PIP_2. These findings indicate that the mode of interactions and conformations of cyt *c* in complex with anionic lipids having different headgroups vary substantially.

Maximal peroxidase activities of cyt *c* in the complex with anionic lipids substantially differ. Thus, TOCL and DOPA

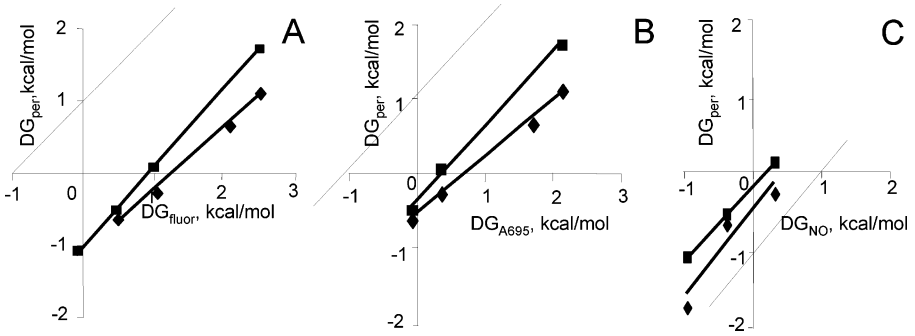

FIGURE 6: Dependence of activation free energies of peroxidase activity of cyt *c* on the stability (free energies of unfolding) of protein domains probed by fluorescence (A), absorbance at 695 nm (B), and heme nitrosylation (C) (kilocalories per mole). Peroxidase activity was probed by etoposide oxidation assay (◆) and Amplex Red oxidation (■).

produced ~3 times higher maximal peroxidase activity than DOPS. These findings suggest that phosphate groups of TOCL and DOPA not only are essential for the binding with Lys residues of cyt *c* but also may additionally have an acid/base catalytic function to assist in splitting of the H_2O_2 molecule by iron. While the latter may be also true for PIP_2 and PIP_3, a lower maximal peroxidase activity of cyt *c* in the complexes with these phospholipids could be due to a smaller scale of their denaturing effects on cyt *c* as evidenced by Trp_{59} fluorescence results. It is likely that a more compact denatured state of the protein leads to a higher effective concentration of histidines and other Fe-coordinating residues that inhibit heme peroxidase activity.

Interestingly, PIP_2 and PIP_3 strongly differed in their ability to induce peroxidase activity and cyt *c* structural changes, although chemically they differ by only a single phosphate group (Figure 1). The activity difference between the two lipids is probably due to the larger negative charge of PIP_3 and stronger electrostatic attraction to positively charged residues of cyt *c*. DOPS and PIP_2 interact with cyt *c* more weakly than DOPA or TOCL. These differences apparently can be attributed to bulky serine and inositol residues in the DOPS and PIP_2 headgroup hindering close interactions of positively charged lysine residues of cyt *c* with negatively charged phosphate groups of the phospholipids. A higher pK_a value (5.5) of titratable carboxylic group in DOPS versus that of the phosphate group of TOCL and DOPA (*3*, *43*−*45*) may also contribute to the relative weakness of DOPS versus TOCL and DOPA. In the membrane, anionic lipids strongly interact electrostatically, and thus, pK_a values of titratable groups shift strongly in the positive direction. As a result, the effective surface charge density of DOPS-containing membranes will likely be lower that that of TOCL- and DOPA-containing membranes, because many DOPS molecules will be neutral in the membrane.

Quantitative Analysis of cyt c Structural Destabilization and Activation of Peroxidase Activity. To quantitatively describe changes in the stability of cyt *c* regions affected by anionic phospholipids, we computed free energies of conformational transitions responsible for spectroscopic changes, ΔG_{fluor} (Trp_{59} fluorescence), ΔG_{A695} (absorbance at 695 nm), and ΔG_{NO} (heme−NO complex formation probed by EPR). Further, we characterized relationships between the induction of peroxidase activity and perturbations of the cyt *c* structure by introducing a two-state model with the open protein state having maximal peroxidase activity, k_{perox}^{max}, the closed state having negligible peroxidase activity, and equilibrium between these two states described by the free energy difference ΔG_{perox}. The mathematical expressions relating ΔG_{fluor}, ΔG_{A695}, ΔG_{NO}, and ΔG_{perox} to the experimental observables can be found in the Appendix.

Upon interaction with anionic liposomes, the structure of cyt *c* destabilizes and activation energies ΔG_{fluor}, ΔG_{A695}, ΔG_{NO}, and ΔG_{perox} are diminished. Figure 6 shows the relationship among ΔG_{fluor}, ΔG_{A695}, ΔG_{NO}, and ΔG_{perox} for interactions of cyt *c* with TOCL/DOPC liposomes at different lipid:protein ratios. It can be seen that the ΔG_{perox} activation energy depends linearly on ΔG_{fluor}, ΔG_{A695}, and ΔG_{NO} with a slope close to 1 (Figure 6), indicating that indeed one can associate peroxidase activity with a specific perturbation of the cyt *c* structure. Interestingly, ΔG_{fluor}, ΔG_{A695}, ΔG_{NO}, and ΔG_{perox}, although strongly correlated, are not identical but shifted relative to each other by a constant. Trp_{59} is located in the "yellow neck" region of cyt *c* in the classification of Englander (*16*, *18*) with a stability energy of 7.4 kcal/mol, while Met_{80} is located in the "red" region with a stability energy of 6.0 kcal/mol. Thus, it is expected that ΔG_{A695} will be smaller than ΔG_{fluor}. The activation energy of the peroxidase reaction, ΔG_{perox}, was found to be ~1 kcal/mol less than the free energy needed to unfold the cyt *c* domain containing Trp_{59} (ΔG_{fluor}). Also, ΔG_{perox} is smaller by 0.3−0.6 kcal/mol than ΔG_{A695}; thus, it is not strictly correct to identify the disruption of the Met_{80}−Fe coordination bond with the peroxidase reaction activation. Peroxidase activity is probably associated with the perturbation of the cyt *c* structure that forms a channel that allows small hydrogen peroxide molecules to reach iron without a complete destabilization of the protein domain containing Met_{80}. Notably, ΔG_{perox} appears to be very close to ΔG_{NO} probably because the process of formation of the heme−NO complex is very similar to the formation of the complex between heme and hydrogen peroxide that is a prerequisite for the catalysis of hydrogen peroxide reduction. A smaller value of ΔG_{perox} activation energy may also reflect destabilization of the cyt *c* structure as a result of oxidation of protein residues during the peroxidase reaction (*46*).

At the lipid:protein ratios that were studied, all cyt *c* molecules are bound to anionic membranes due to strong electrostatic interactions at the low ionic strength used in the experiments. Dynamic equilibrium exists between native cyt *c* molecules and those denatured by lipid structures. cyt *c* in the denatured state occupies a much larger surface area

than in the native state; therefore, an increase in the accessible lipid surface shifts the equilibrium toward the denatured state. At high lipid:protein ratios, the quantity $RT \ln(c_{lipid}/mc_{prot})$, where m is the number of lipid molecules in complex with a denatured cyt *c* molecule characterizing the entropy part of the free energy of the cyt *c* denatured by a lipid membrane. One can expect that stabilization energies of cyt *c* domains will be reduced in parallel with an increase in $RT \ln(c_{lipid}/mc_{prot})$; indeed, we observed (not shown) a linear dependence of ΔG_{fluor}, ΔG_{A695}, ΔG_{NO}, and ΔG_{perox} as a function of $RT \ln(c_{lipid}/mc_{prot})$ with a slope of $\sim$1.

Role of cyt c Peroxidase Activity in Peroxidation of Anionic Phospholipids in Cells. Our structural studies in model systems established the effectiveness of anionic phospholipids in inducing destabilization of the cyt *c* protein structure. Hierarchical ranking indicates that assessment of NO binding is a more accurate criterion for characterizing the potency of anionic phospholipids as inducers of the peroxidase activity in in vitro models than the other two assays that were studied. Previous work by us and others has emphasized the importance of hydrophobic interactions as determinants, along with electrostatic forces, in inducing cyt *c* unfolding and activation of its peroxidase activity not only with synthetic chemical substrates but also toward peroxidation of natural substrates such as CL and PS (*9*, *21*, *42*). This may be particularly important in cells, where the presence of anionic phospholipids in sufficient concentrations, their topography, and the mutual proximity of phospholipids and cyt *c* may play a very substantial role. To estimate the peroxidase function of cyt *c* in vivo, we experimentally assessed peroxidation of polyunsaturated anionic phospholipids in wild-type HeLa cells with a full complement of cyt *c* and cyt *c*-deficient HeLa 1.2 cells. Our MS analyses confirmed that molecular species of major anionic phospholipids were not significantly different between the two types of cells, suggesting that differences in the random oxidizability of these polyunsaturated substrates could not play any role in observed specific features of their oxidation. Only two anionic phospholipids, CL and PS, were oxidized in wild-type HeLa cells but not in cyt *c*-deficient HeLa 1.2 cells. More abundant but noncharged phospholipids, PC and PE, did not undergo peroxidation in either HeLa cells or HeLa 1.2 cells. Similarly, triggering of apoptosis by a nonoxidant, ActD, in cyt $c^{+/+}$ MECs caused selective peroxidation of anionic phospholipids, among which CL and PS were the major oxidation substrates along with some oxidation of PI. In cyt *c*-deficient MECs, oxidation of these anionic phospholipids did not happen in spite of sufficient amounts of their polyunsaturated oxidizable molecular species and adequate ActD-induced production of reactive oxygen species.

There are two conclusions from these findings. The first one is that cyt *c* indeed acts as a peroxidase under physiological conditions, and its presence is required for the catalysis of peroxidation of anionic phospholipids. The second one is that the order of effectiveness of anionic phospholipids in inducing the peroxidase activity of cyt *c* whereby CL > PS holds true for phospholipid peroxidation in cells. PA is not found in cells in any significant amounts and, hence, cannot participate in cyt *c*-catalyzed peroxidation reactions. Notably, CL is a mitochondrion-specific phospholipid, while PS is found in extramitochondrial locations (*47*). This suggests that the peroxidase activity of cyt *c* was realized in two different cell compartments. On the basis of our previous studies with pro-apoptotic stimulation of cells, it is likely that oxidation of CL occurred very early during the development of the apoptotic program when the majority of cyt *c* was still confined to mitochondria, whereas PS oxidation took place after the release of cyt *c* from mitochondria into the cytosol. It is possible that PS on the inner leaflet of the plasma membrane is a preferred substrate for the interactions with cytosolic cyt *c*. It is important to note that externalization of PS on the surface of the plasma membrane is one of the hallmarks of apoptosis that generates "eat-me" signals on the surface of apoptotic cells, PS and oxidized PS. These signals are recognized by professional phagocytes and are essential for clearance of apoptotic cells via phagocytotic pathways and regulation of inflammatory response (*8*, *26*).

While different PI species are found in cells in total amounts comparable to those of CL and PS, their distribution between organelles and between the inner and outer leaflets of membranes does not favor the interactions of PIs with cyt *c*. PI is present in almost equal amounts in different organelles: mitochondria, microsomes, plasma membrane, Golgi apparatus, and lysosomes (*47*). In contrast, CL is found only in mitochondria especially in the inner leaflet of the inner mitochondrial membrane, while PS is common to plasma membranes, Golgi apparatus, and microsomes (*47*). Seven phosphoinositide species of PI can be found in cells due to reversible phosphorylation of its inositol ring at positions 3, 4, and 5. PIP_4 and 4,5-PIP_2 represent the bulk of these lipids in mammalian cells, while other phosphoinositides are generally less abundant by 1 order of magnitude (*26*, *47*).

One may wonder why CL, so effective in converting cyt *c* into a peroxidase, is abundant in mitochondria while PS, much less potent as an inducer of cyt *c* peroxidase activity, is completely lacking in mitochondria (*47*). CL is highly compartmentalized in mitochondria and confined to parts of the inner membrane where it has only limited access to cyt *c* in the intermembrane space. Normally, four hydrophobic fatty acyls and two negative charges limit transmembrane migrations of CL in mitochondria and its possible interactions with cyt *c*. PS, on the other hand, is known to readily undergo spontaneous transbilayer movements (*49*). Not surprisingly, aminophospholipid translocase activity is critical to the maintenance of PS asymmetry (with remarkable prevalence in the inner leaflet) in the plasma membrane (*49*, *50*). Thus, it is possible that any presence of PS in mitochondria would be detrimental to their functions due to likely formation of cyt *c*−PS complexes and peroxidase-induced damage of the organelles.

The propensity of CL to cause destabilization of nonbilayer membrane arrangements (*51*, *52*) may be associated with its important pro-apoptotic functions. It is tempting to speculate that CL peroxidation products, formed by cyt *c* peroxidase activity, are essential components of these structural rearrangements associated with the release of pro-apoptotic factors from mitochondria.

Overall, our findings in cells confirm our conclusions about the structural hierarchy of interactions of cyt *c*

peroxidase with anionic phospholipids, particularly CL and PS, and contribute significantly to the understanding of the physiological role of these mechanisms in regulation of the apoptotic program in mitochondria and apoptotic clearance of cells through recognition of an eat-me signal, externalized PS and its oxidation products. Structural domains capable of binding anionic phospholipids are typical of a number of peripheral proteins (e.g., annexins, synucleins, and protein kinases) in different cells. A number of peripheral membrane proteins (phospholipases, lipoxygenases, and others), similar to cyt *c*, change conformation and activate catalytic properties upon binding to anionic membranes. Elucidation of their specific lipid binding sites and consequences of the protein−lipid interactions may be instrumental in the discovery of new functions and control mechanisms of these proteins in cellular processes. Further understanding of apoptotic functions and mechanisms of Bcl-2 family members, particularly Bax and tBid, may also be stimulated by clarification of their interactions with anionic CL and its metabolism (*53*−*55*).

APPENDIX

To describe quantitatively changes in the stability of the protein regions under the influence of anionic lipids, we can introduce free energies of conformational transitions responsible for spectroscopical changes, ΔG_{fluor}, ΔG_{A695}, and ΔG_{NO}.

We may represent the unfolding process as an F ↔ U reaction with the equilibrium constant K (=[U]/[F]), where F and U are folded and unfolded states, respectively. From experimental data, we can calculate K. For example, under the assumption that the fluorescence intensity of the folded state of cyt *c* is negligible and is equal to $fluor_{max}$ when the region of the protein containing Trp_{59} is unfolded, K can be found as

$$K = \frac{\text{fluor}}{\text{fluor}_{max} - \text{fluor}}$$

where fluor is the observed fluorescence intensity. Then the free energy of unfolding associated with a protein domain containing Trp_{59} can be found as

$$\Delta G_{fluor} = -RT \ln K \tag{A1}$$

where ΔG_{fluor} is the free energy of unfolding of the protein region containing the Trp_{59} residue, R (8.31 J/K) is the gas constant, and T is the absolute temperature in kelvin.

Analogously, activation of optical absorption at 695 nm can be described by activation free energy ΔG_{A695}:

$$\Delta G_{A695} = -RT \ln \frac{A_{695}^{max} - A_{695}}{A_{695}^{max}} \tag{A2}$$

where ΔG_{A695} is the free energy associated with the protein structure perturbation that disrupts the Fe−S(Met_{80}) bond and A_{695}^{max} is the 695 nm absorbance of the cyt *c* in the native conformation.

The observed amplitude of the EPR signal of NO complexes can be characterized by activation free energy ΔG_{NO}:

$$\Delta G_{NO} = -RT \ln \frac{\text{EPR}}{\text{EPR}_{NO}^{max} - \text{EPR}} \tag{A3}$$

where EPR_{NO}^{max} is the maximal amplitude of the EPR signal of the heme−NO complex (unfolded cyt *c* at saturating nitric oxide concentrations).

The induction of cyt *c* peroxidase activity strongly correlated with the destabilization of the tertiary structure of the protein, and we can hypothesize that an access of hydrogen peroxide molecule to the catalytic Fe atom is associated with a particular perturbation of the cyt *c* structure that allows the access of the hydrogen peroxide molecule to the catalytic metal atom. This perturbation may include the disruption of the Fe−S(Met_{80}) coordination bond and formation of the channel in the protein to allow access of the hydrogen peroxide molecule to the metal atom. We can introduce free energy ΔG_{perox} needed to form an access channel for the hydrogen peroxide molecule that is associated with a probability p_{perox} for opening the channel as

$$p_{perox} = \frac{\exp\left(-\frac{\Delta G_{perox}}{k_B T}\right)}{1 + \exp\left(-\frac{\Delta G_{perox}}{k_B T}\right)} \tag{A4}$$

Assuming that the peroxidase activity of cyt *c* is maximal with k_{perox}^{max} when the hydrogen peroxide access channel is formed and zero if no channel is present, the peroxidase rate constant can be expressed as

$$k_{perox} = k_{perox}^{max} p_{perox} = k_{perox}^{max} \frac{\exp\left(-\frac{\Delta G_{perox}}{k_B T}\right)}{1 + \exp\left(-\frac{\Delta G_{perox}}{k_B T}\right)} \tag{A5}$$

and the activation energy of peroxidase reaction can be expressed as

$$\Delta G_{perox} = -k_B T \ln\left(\frac{k_{perox}}{k_{perox}^{max} - k_{perox}}\right) \tag{A6}$$

REFERENCES

1. Walsh, C. T. (2006) *Posttranslational modification of proteins: Expending nature's inventory*, Roberts and Co. Publishers.
2. Cho, W., and Stahelin, R. V. (2005) Membrane-protein interactions in cell signaling and membrane trafficking, *Annu. Rev. Biophys. Biomol. Struct. 34*, 119−151.
3. Sanderson, J. M. (2005) Peptide-lipid interactions: Insights and perspectives, *Org. Biomol. Chem. 3*, 201−212.
4. Tamm, L. K., Ed. (2005) *Protein-Lipid Interactions: From Membrane Domains to Cellular*, Wiley, New York.
5. Ott, M., Gogvadze, V., Orrenius, S., and Zhivotovsky, B. (2007) Mitochondria, oxidative stress and cell death, *Apoptosis 12*, 913−922.
6. Gonzalvez, F., and Gottlieb, E. (2007) Cardiolipin: Setting the beat of apoptosis, *Apoptosis 12*, 877−885.
7. Rytomaa, M., and Kinnunen, P. K. (1995) Reversibility of the binding of cytochrome c to liposomes. Implications for lipid-protein interactions, *J. Biol. Chem. 270*, 3197−3202.
8. Nantes, I. L., Zucchi, M. R., Nascimento, O. R., and Faljoni-Alario, A. (2001) Effect of heme iron valence state on the conformation of cytochrome c and its association with membrane interfaces. A CD and EPR investigation, *J. Biol. Chem. 276*, 153−158.

9. Belikova, N. A., Vladimirov, Y. A., Osipov, A. N., Kapralov, A. A., Tyurin, V. A., Potapovich, M. V., Basova, L. V., Peterson, J., Kurnikov, I. V., and Kagan, V. E. (2006) Peroxidase activity and structural transitions of cytochrome c bound to cardiolipin-containing membranes, *Biochemistry 45*, 4998−5009.
10. Kagan, V. E., Tyurin, V. A., Jiang, J., Tyurina, Y. Y., Ritov, V. B., Amoscato, A. A., Osipov, A. N., Belikova, N. A., Kapralov, A. A., Kini, V., Vlasova, I. I., Zhao, Q., Zou, M., Di, P., Svistunenko, D. A., Kurnikov, I. V., and Borisenko, G. G. (2005) Cytochrome c acts as a cardiolipin oxygenase required for release of proapoptotic factors, *Nat. Chem. Biol. 1*, 223−232.
11. Maity, H., Maity, M., and Englander, S. W. (2004) How cytochrome c folds, and why: Submolecular foldon units and their stepwise sequential stabilization, *J. Mol. Biol. 343*, 223−233.
12. Berners-Price, S. J., Bertini, I., Gray, H. B., Spyroulias, G. A., and Turano, P. (2004) The stability of the cytochrome c scaffold as revealed by NMR spectroscopy, *J. Inorg. Biochem. 98*, 814−823.
13. Naeem, A., and Khan, R. H. (2004) Characterization of molten globule state of cytochrome c at alkaline, native and acidic pH induced by butanol and SDS, *Int. J. Biochem. Cell Biol. 36*, 2281−2292.
14. Varhac, R., Antalik, M., and Bano, M. (2004) Effect of temperature and guanidine hydrochloride on ferrocytochrome c at neutral pH, *J. Biol. Inorg. Chem. 9*, 12−22.
15. Wen, X., Patel, K. M., Russell, B. S., and Bren, K. L. (2007) Effects of heme pocket structure and mobility on cytochrome c stability, *Biochemistry 46*, 2537−2544.
16. Maity, H., Maity, M., Krishna, M. M., Mayne, L., and Englander, S. W. (2005) Protein folding: The stepwise assembly of foldon units, *Proc. Natl. Acad. Sci. U.S.A. 102*, 4741−4746.
17. Krishna, M. M., Maity, H., Rumbley, J. N., Lin, Y., and Englander, S. W. (2006) Order of steps in the cytochrome C folding pathway: Evidence for a sequential stabilization mechanism, *J. Mol. Biol. 359*, 1410−1419.
18. Maity, H., Rumbley, J. N., and Englander, S. W. (2006) Functional role of a protein foldon: An omega-loop foldon controls the alkaline transition in ferricytochrome c, *Proteins 63*, 349−355.
19. Diederix, R. E., Ubbink, M., and Canters, G. W. (2002) Peroxidase activity as a tool for studying the folding of c-type cytochromes, *Biochemistry 41*, 13067−13077.
20. de Jongh, H. H., Ritsema, T., and Killian, J. A. (1995) Lipid specificity for membrane mediated partial unfolding of cytochrome c, *FEBS Lett. 360*, 255−260.
21. Chattopadhyay, K., and Mazumdar, S. (2003) Stabilization of partially folded states of cytochrome c in aqueous surfactant: Effects of ionic and hydrophobic interactions, *Biochemistry 42*, 14606−14613.
22. Sanghera, N., and Pinheiro, T. J. (2000) Unfolding and refolding of cytochrome c driven by the interaction with lipid micelles, *Protein Sci. 9*, 1194−1202.
23. Pinheiro, T. J., Elove, G. A., Watts, A., and Roder, H. (1997) Structural and kinetic description of cytochrome c unfolding induced by the interaction with lipid vesicles, *Biochemistry 36*, 13122−13132.
24. Pinheiro, T. J., Cheng, H., Seeholzer, S. H., and Roder, H. (2000) Direct evidence for the cooperative unfolding of cytochrome c in lipid membranes from H−^{2}H exchange kinetics, *J. Mol. Biol. 303*, 617−626.
25. Tuominen, E. K., Wallace, C. J., and Kinnunen, P. K. (2002) Phospholipid-cytochrome c interaction: Evidence for the extended lipid anchorage, *J. Biol. Chem. 277*, 8822−8826.
26. Kagan, V. E., Borisenko, G. G., Tyurina, Y. Y., Tyurin, V. A., Jiang, J., Potapovich, A. I., Kini, V., Amoscato, A. A., and Fujii, Y. (2004) Oxidative lipidomics of apoptosis: Redox catalytic interactions of cytochrome c with cardiolipin and phosphatidylserine, *Free Radical Biol. Med. 37*, 1963−1985.
27. Kikuchi, S., Shibuya, I., and Matsumoto, K. (2000) Viability of an *Escherichia coli* pgsA null mutant lacking detectable phosphatidylglycerol and cardiolipin, *J. Bacteriol. 182*, 371−376.
28. Folch, J., Lees, M., and Sloane Stanley, G. H. (1957) A simple method for the isolation and purification of total lipides from animal tissues, *J. Biol. Chem. 226*, 497−509.
29. Kagan, V. E., Ritov, V. B., Tyurina, Y. Y., and Tyurin, V. A. (1998) Sensitive and specific fluorescent probing of oxidative stress in different classes of membrane phospholipids in live cells using metabolically integrated cis-parinaric acid, *Methods Mol. Biol. 108*, 71−87.
30. Chalvardjian, A., and Rudnicki, E. (1970) Determination of lipid phosphorus in the nanomolar range, *Anal. Biochem. 36*, 225−226.
31. Tsong, T. Y. (1976) Ferricytochrome c chain folding measured by the energy transfer of tryptophan 59 to the heme group, *Biochemistry 15*, 5467−5473.
32. Droghetti, E., Oellerich, S., Hildebrandt, P., and Smulevich, G. (2006) Heme coordination states of unfolded ferrous cytochrome C, *Biophys. J. 91*, 3022−3031.
33. Vlasova, I. I., Tyurin, V. A., Kapralov, A. A., Kurnikov, I. V., Osipov, A. N., Potapovich, M. V., Stoyanovsky, D. A., and Kagan, V. E. (2006) Nitric oxide inhibits peroxidase activity of cytochrome c·cardiolipin complex and blocks cardiolipin oxidation, *J. Biol. Chem. 281*, 14554−14562.
34. de Sanctis, D., Pesce, A., Nardini, M., Bolognesi, M., Bocedi, A., and Ascenzi, P. (2004) Structure-function relationships in the growing hexa-coordinate hemoglobin sub-family, *IUBMB Life 56*, 643−651.
35. Ehrenshaft, M., and Mason, R. P. (2006) Protein radical formation on thyroid peroxidase during turnover as detected by immuno-spin trapping, *Free Radical Biol. Med. 41*, 422−430.
36. Qian, S. Y., Chen, Y. R., Deterding, L. J., Fann, Y. C., Chignell, C. F., Tomer, K. B., and Mason, R. P. (2002) Identification of protein-derived tyrosyl radical in the reaction of cytochrome c and hydrogen peroxide: Characterization by ESR spin-trapping, HPLC and MS, *Biochem. J. 363*, 281−288.
37. Detweiler, C. D., Lardinois, O. M., Deterding, L. J., de Montellano, P. R., Tomer, K. B., and Mason, R. P. (2005) Identification of the myoglobin tyrosyl radical by immuno-spin trapping and its dimerization, *Free Radical Biol. Med. 38*, 969−976.
38. Keszler, A., Mason, R. P., and Hogg, N. (2006) Immuno-spin trapping of hemoglobin and myoglobin radicals derived from nitrite-mediated oxidation, *Free Radical Biol. Med. 40*, 507−515.
39. Chen, Y. R., Deterding, L. J., Sturgeon, B. E., Tomer, K. B., and Mason, R. P. (2002) Protein oxidation of cytochrome C by reactive halogen species enhances its peroxidase activity, *J. Biol. Chem. 277*, 29781−29791.
40. Chen, Y. R., Chen, C. L., Chen, W., Zweier, J. L., Augusto, O., Radi, R., and Mason, R. P. (2004) Formation of protein tyrosine ortho-semiquinone radical and nitrotyrosine from cytochrome c-derived tyrosyl radical, *J. Biol. Chem. 279*, 18054−18062.
41. Svistunenko, D. A. (2005) Reaction of haem containing proteins and enzymes with hydroperoxides: The radical view, *Biochim. Biophys. Acta 1707*, 127−155.
42. Tyurina, Y. Y., Kini, V., Tyurin, V. A., Vlasova, I. I., Jiang, J., Kapralov, A. A., Belikova, N. A., Yalowich, J. C., Kurnikov, I. V., and Kagan, V. E. (2006) Mechanisms of cardiolipin oxidation by cytochrome c: Relevance to pro- and antiapoptotic functions of etoposide, *Mol. Pharmacol. 70*, 706−717.
43. Fisar, Z. (2005) Interactions between tricyclic antidepressants and phospholipid bilayer membranes, *Gen. Physiol. Biophys. 24*, 161−180.
44. Haines, T. H., and Dencher, N. A. (2002) Cardiolipin: A proton trap for oxidative phosphorylation, *FEBS Lett. 528*, 35−39.
45. Marsh, D. (1990) *CRC Handbook of Lipid Bilayers*, CRC Press, Boca Raton, FL.
46. Basova, L. V., Kurnikov, I. V., Wang, L., Ritov, V. B., Belikova, N. A., Vlasova, I. I., Pacheco, A. A., Winnica, D. E., Peterson, J., Bayir, H., Waldeck, D. H., and Kagan, V. E. (2007) Cardiolipin switch in mitochondria: Shutting off the reduction of cytochrome c and turning on the peroxidase activity, *Biochemistry 46*, 3423−3434.
47. Vance, J. E., and Steenbergen, R. (2005) Metabolism and functions of phosphatidylserine, *Prog. Lipid Res. 44*, 207−234.
48. Wu, Y., Tibrewal, N., and Birge, R. B. (2006) Phosphatidylserine recognition by phagocytes: A view to a kill, *Trends Cell Biol. 16*, 189−197.
49. Balasubramanian, K., and Schroit, A. J. (2003) Aminophospholipid asymmetry: A matter of life and death, *Annu. Rev. Physiol. 65*, 701−734.
50. Daleke, D. L. (2003) Regulation of transbilayer plasma membrane phospholipid asymmetry, *J. Lipid Res. 44*, 233−242.
51. Nichols-Smith, S., Teh, S. Y., and Kuhl, T. L. (2004) Thermodynamic and mechanical properties of model mitochondrial membranes, *Biochim. Biophys. Acta 1663*, 82−88.
52. Ortiz, A., Killian, J. A., Verkleij, A. J., and Wilschut, J. (1999) Membrane fusion and the lamellar-to-inverted-hexagonal phase

transition in cardiolipin vesicle systems induced by divalent cations, *Biophys. J. 77*, 2003−2014.
53. Van Mau, N., Kajava, A. V., Bonfils, C., Martinou, J. C., and Harricane, M. C. (2005) Interactions of Bax and tBid with lipid monolayers, *J. Membr. Biol. 207*, 1−9.
54. Gonzalvez, F., Pariselli, F., Dupaigne, P., Budihardjo, I., Lutter, M., Antonsson, B., Diolez, P., Manon, S., Martinou, J. C., Goubern, M., Wang, X., Bernard, S., and Petit, P. X. (2005) tBid interaction with cardiolipin primarily orchestrates mitochondrial dysfunctions and subsequently activates Bax and Bak, *Cell Death Differ. 12*, 614−626.
55. Tyurin, V. A., Tyurina, Y. Y., Osipov, A. N., Belikova, N. A., Basova, L. V., Kapralov, A. A., Bayir, H., and Kagan, V. E. (2007) Interactions of cardiolipin and lyso-cardiolipins with cytochrome c and tBid: Conflict or assistance in apoptosis, *Cell Death Differ. 14*, 872−875.

BI701237B